



**HAL**  
open science

## Patterned PPy Polymer and PPy/Ag Nanocomposites Thin Films by Photo-DLICVD

Claudiu Constantin Manole, Francis Maury, Ioana Demetrescu

► **To cite this version:**

Claudiu Constantin Manole, Francis Maury, Ioana Demetrescu. Patterned PPy Polymer and PPy/Ag Nanocomposites Thin Films by Photo-DLICVD. *Physics Procedia*, 2013, vol. 46, pp. 46-55. 10.1016/j.phpro.2013.07.044 . hal-01172381

**HAL Id: hal-01172381**

**<https://hal.science/hal-01172381>**

Submitted on 7 Jul 2015

**HAL** is a multi-disciplinary open access archive for the deposit and dissemination of scientific research documents, whether they are published or not. The documents may come from teaching and research institutions in France or abroad, or from public or private research centers.

L'archive ouverte pluridisciplinaire **HAL**, est destinée au dépôt et à la diffusion de documents scientifiques de niveau recherche, publiés ou non, émanant des établissements d'enseignement et de recherche français ou étrangers, des laboratoires publics ou privés.



## Open Archive TOULOUSE Archive Ouverte (OATAO)

OATAO is an open access repository that collects the work of Toulouse researchers and makes it freely available over the web where possible.

This is an author-deposited version published in : <http://oatao.univ-toulouse.fr/>  
Eprints ID : 14105

**To link to this article** : doi: 10.1016/j.phpro.2013.07.044  
URL : <http://dx.doi.org/10.1016/j.phpro.2013.07.044>

<p><b>To cite this version</b> : Manole, Claudiu Constantin and Maury, Francis and Demetrescu, Ioana <i>Patterned PPy Polymer and PPy/Ag Nanocomposites Thin Films by Photo-DLICVD</i>. (2013) <i>Physics Procedia</i>, vol. 46. pp. 46-55. ISSN 1875-3892</p>
--

Any correspondence concerning this service should be sent to the repository administrator: [staff-oatao@listes-diff.inp-toulouse.fr](mailto:staff-oatao@listes-diff.inp-toulouse.fr)

Nineteenth European Conference on Chemical Vapor Deposition, (EUROCV D 19)

# Patterned PPy Polymer and PPy/Ag Nanocomposites Thin Films by Photo-DLICVD

C.C. Manole<sup>a,b\*</sup>, F. Maury<sup>a</sup>, I. Demetrescu<sup>b</sup>

<sup>a</sup>CIRIMAT, CNRS/INPT/UPS, 4 allée E. Monso, BP 44362, 31030 Toulouse cedex 4, France

<sup>b</sup>UPB, Faculty of Applied Chemistry and Materials Science, 1-7 Polizu 011061, Bucharest, Romania

---

## Abstract

This work deals with the deposition of both undoped (insulator) and extrinsically Ag-doped (conductive) polypyrrole (PPy) coatings by an original Photo-DLICVD process. The uniform and conformal coverage of PPy thin films on both Si(100) wafer and liquid micro-droplets forming blisters is investigated. A self-ordered surface patterning of the blisters is achieved and discussed in relation with the substrate nature. By changing the precursor chemistry in this CVD process, conductive PPy/Ag nanocomposite films are grown. First evidence for conductive behavior of these Ag-doped PPy coatings was found. The Ag nanoparticles (NPs) reveal 1D assembly at the ledges of crystal-like facets of micron size nanocomposite particles leading to more complex arrangements of the metal NPs in the hybrid PPy/Ag coatings.

---

## 1. Introduction

The Chemical Vapor Deposition (CVD) is a powerful process used to deposit conformal thin films with a wide range of applications (Jones and Hitchman, 2009). The deposition occurs from a reactive gas phase formed by vaporizing a liquid or solid precursor which is transported by convection with a carrier gas. This vapor phase reacts chemically to form a thin film on the substrate. The molecular precursors provide the

---

\* Corresponding author. Tel.: +0-000-000-0000 ; fax: +0-000-000-0000 .  
E-mail address: claudiuconstantin.manole@ensiacet.fr.

chemical elements necessary for the growth of the desired metal, semiconductor, ceramic or polymer thin films (Park, 2001). The transition from the condensed state to the vapor phase can be achieved by various CVD technologies such as sublimation of powder (Santucci et al., 2010), bubbling through a liquid (Chan et al., 2006) and aerosol-assisted methods (Bakar et al., 2012; Crick et al., 2012; Edusi et al., 2012; Shah et al., 2012). This paper deals with a particular method to form the vapor phase from a liquid precursor, namely the pulsed Direct Liquid Injection (DLI). By this method many oxides (Weiss et al., 2000; Douard and Maury, 2006; Mungkalasiri et al., 2009) but also non oxide ceramic coatings (Boisselier et al., 2013) as metal carbides, nitrides (Maury et al., 2009) and nanostructured coatings (Maury et al., 2009) were obtained at temperatures above 600 K and under either atmospheric pressure (Maury et al., 2009) or moderately reduced pressure (Douard et al., 2008). The use of a DLI system adds versatility to the CVD processes by the possibility to use wet chemistry methods to prepare the precursor solution which can be subsequently transformed into vapor phase.

This offers the premises of using the DLI system for the deposition of polymers, especially in the context of the growing CVD research in this area (Malinauskas, 2001; Santucci et al., 2010; Ozaydin-Ince et al., 2012; Xu et al., 2012). The parameters that control the polymer growth can be either physical (*e.g.* the pressure and the temperature) or chemical (*e.g.* the chemical reactions and their kinetics). Physically, as the substrate temperature decreases, the adsorption of the monomers on the surface increases (Ozaydin-Ince and Gleason, 2010). This generally leads to an increase of the growth rate. For instance at temperatures as low as 208 K we observed increases of deposition rates for poly(methyl methacrylate) (PMMA) films that confirms the increased adsorption (Manole et al., 2012). Another physical manner to control the deposition can be achieved by changing the total pressure in the CVD reactor, as described to adjust the properties of pentacene films (Ahn et al., 2003, 2012). In this work, changes in the precursor chemistry were investigated.

We report the early results of a comprehensive program dealing with CVD of doped and undoped polymer thin films. After some works on parylen (Santucci et al., 2010) and PMMA (Manole et al., 2012) this paper focus on an original CVD process to grow PPy thin films.

The PPy was first obtained in 1916 by oxidation of the monomer with hydrogen peroxide as “polypyrrole black” amorphous powder (Angeli and Alessandri, 1916). In 1968 the electrochemical synthesis of PPy was reported (Dall’Olio et al., 1968), while in 1979 the electrochemical technique was optimized to obtain high conductive PPy (Diaz et al., 1979). The growth of the PPy films by the CVD technique dates back to 1986, when PPy films with properties similar to those obtained by electrochemical techniques are reported (Mohammadi et al., 1986).

This paper follows the path of tailoring the film properties and of increasing the polymerization efficiency by extrinsic Ag doping. The PPy films are deposited simultaneously with Ag nanoparticles (NPs) from the same monomer solution by an original Direct Liquid Injection (DLI) CVD to obtain extrinsically Ag-doped PPy films. The polymerization is achieved by UV irradiation of monomer in the gas phase, through a process described as photon-assisted DLICVD (Photo-DLICVD). Furthermore, based on previous results that revealed monomer encapsulation in PMMA films at specific nucleation sites (Manole et al., 2012), we explore aspects that relate to the heterogeneous nucleation at the substrate level. This offers the premises of a controlled surface patterning of the PPy films by self-ordering of blisters. The process is also used for the deposition of PPy/Ag NPs composite films with crystal-like facet morphology.

## 2. Materials and methods

The photo-DLICVD is composed of 6 key elements: (i) a pressurized precursor reservoir, (ii) the DLI system, (iii) the vaporization zone, (iv) the UV chamber, (v) the deposition reactor and (vi) the exhaust equipments including a liquid nitrogen trap, a vacuum pump and an automatic pressure control system. The

components (ii), (iii), (iv), and (v), *i.e.* the vaporization, activation and deposition zones, are vertically aligned (equiaxed geometry). For the two series of runs, *i.e.* for undoped and doped polymer films, the injected precursor was composed of pyrrole (Py) as liquid monomer source with 2 % of 1-hydroxycyclohexyl phenyl ketone (HCHPK) as photo initiator and, only for doped films, silver nitrate was dissolved in this solution with a Py:AgNO<sub>3</sub> mole ratio of 50:1 with 3% HCHPK, all from Sigma Aldrich. All compounds were store in the dark at about 277 K (in a refrigerator) and the precursor solutions were prepared only a few minutes prior their use.

A Kemstream DLI system composed of a liquid injector that communicates with a mixing chamber was used. The reservoir of liquid precursor was pressurized under N<sub>2</sub> at  $P_l = 350$  kPa. For these experiments, the opening time of the injector was  $t_{on} = 1$  ms and the repeating frequency of this process was  $f = 10$  Hz. In the mixing chamber the liquid is mixed with N<sub>2</sub> as carrier gas. The liquid/gas mixture is flash vaporized in the vaporization chamber in a pulsed manner by a N<sub>2</sub> motive pressure of  $P_g = 200$  kPa and N<sub>2</sub> gas flow of 150 sccm with the frequency of 1 Hz. The UV chamber consists of a quartz tube where the gas phase is irradiated by 4 UV lamps of 20 W each with a peak irradiance of 150  $\mu\text{W}/\text{cm}^2$  (at a distance of 1 m) at 254 nm. The depositions were made at room temperature under a total pressure of  $P_T = 1.27$  kPa. The substrates (glass and Si(100) wafer) were prepared by a careful process of degreasing (mechanical cleaning with ethanol and acetone), ultrasonication (5 + 5 min with acetone and ethanol, respectively), rinsing (ethanol then acetone) and Ar gas drying.

The Atomic Force Microscopy (AFM) and Spectroscopy (AFS) were made with an Agilent Technology 5500 AFM. The FESEM micrographs were obtained with a JEOL JSM-6700F Field Emission Scanning Electron Microscope. Raman spectra were obtained with Horiba LabRAM Confocal Spectrometer that emits at 532 nm. A Siefert XRD 3003 TT X-ray diffraction system with a Cu K $\alpha$  radiation (1.542 Å) was used for XRD measurements.

### 3. Results and discussion

This work aims a chemical approach to change the properties of PPy thin films from insulator to electrical conductor. More precisely, this paper reports an original CVD process for the growth of PPy and Ag-doping of these thin films. A single liquid solution containing all the reactants was injected and photo-activation of the gas phase (without irradiation of the substrate) produced the reactive species necessary for the growth of the polymeric films. For all CVD runs, the deposition occurs at room temperature.

#### 3.1. Undoped PPy films

The PPy films were obtained from a precursor solution of Py monomer and 2% HCHPK. From a general point of view, the characterization of organic polymer films which are both insulator and very thin (less than a few hundred nanometers) is difficult. Here Atomic Force Spectroscopy (AFS) measurements were made to investigate the conformal coverage of PPy after deposition. During the AFS measurements, the AFM tip interacts with the sample by an approach/retract cycle. The linear-elastic interaction of each material is proportional to the time it takes for AFM tip to interact with the sample. For the surface of a bare Si(100) substrate with its native oxide, noted as reference in *Figure 1b*, it takes 0.3 s for the AFM tip to reach and to retract from the surface (data given by the width of the base of the peak). When the AFM tip interacts with the coated sample, it takes 1.9 s to complete the cycle. The time is the same for the AFS over a flat and smooth surface (point 2 in *Figure 1*) and over a heterogeneity that looks like a blister (point 1 in *Figure 1*). This confirms a good conformal coverage with PPy of the same elasticity. This blister of micrometric size contains

most likely unreacted liquid Py monomer inside, as previously reported for PMMA in similar CVD conditions (UV activation of gas phase, low pressure, room temperature) (Manole et al., 2012).

SEM observations using an acceleration voltage higher than 5 kV left traces on the images when the magnification was changed rapidly or the sample was moved. This is characteristic of an insulator material which accumulates the electrical charges (afterimage). Further SEM analyses were conducted at lower voltage.

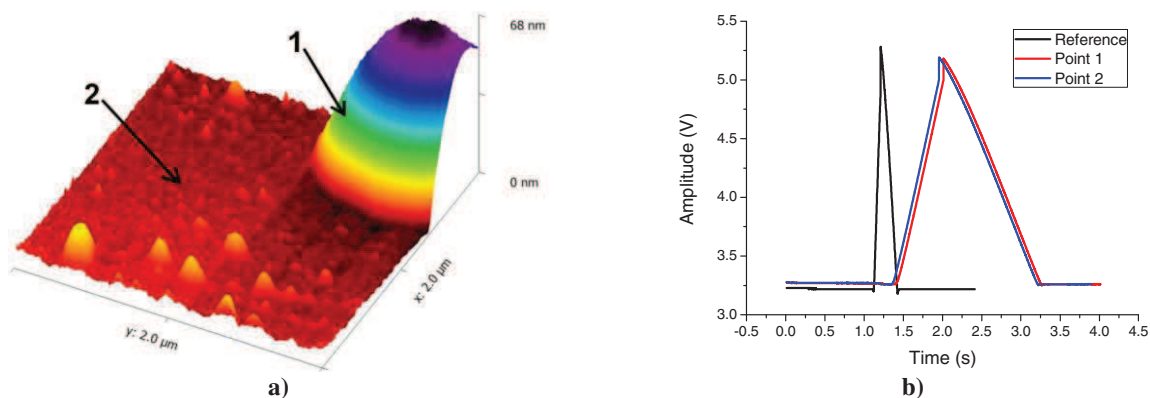


Figure 1: AFM analysis: (a) AFM micrograph showing two points over the deposited PPy film grown on Si(100) where the AFS measurements were obtained; (b) AFS spectra of these two points and of the bare Si(100) substrate given as reference.

After the deposition, blisters of approximately 15-20  $\mu\text{m}$  in diameter are observed in the FESEM micrograph (Figure 2). Interestingly the shape and the size distribution of the blisters is indicative of the processes that occur at the surface of the Si(100) substrate in the early stages of the growth.

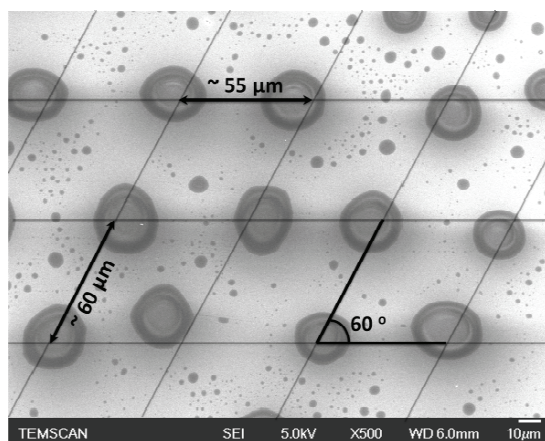


Figure 2: FESEM image of the PPy film grown on Si(100) substrate with encapsulated self-ordered blisters. A grid pattern has been drawn on the picture to show the geometrical features of the pattern formed by the self-ordered blisters.

In the CVD of polymers, the elementary processes that are considered to be involved in the early deposition stages are: (i) a first step of adsorption, (ii) followed by lateral diffusion of the molecules, (iii) then by surface reactions as polymerization in this case (Park, 2001). The sites of heterogeneous reactions are (iv)

centers of nucleation and they lead to (v) the subsequent growth and formation of a continuous film (Park, 2001). The nucleation occurs preferentially at heterogeneities on the surface, also called heterogeneous nucleation. For instance the heterogeneous nucleation is used to control the growth of NPs at surface defects deliberately made (Cao, 2004).

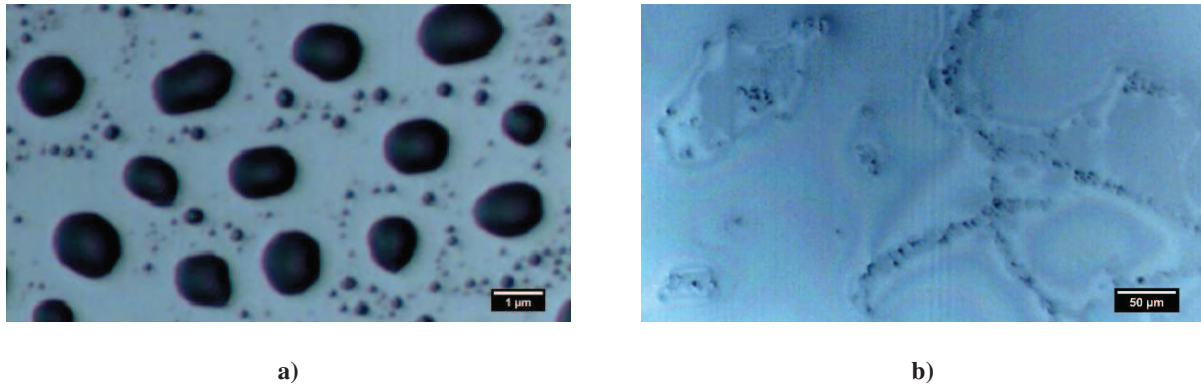


Figure 3: Optical microscope images of PPy blisters deposited a) self-ordered on Si(100) substrate and b) disordered on glass substrate

For the PPy deposition, the Si(100) wafer was used without any pretreatment required to deliberately control the crystallographic structure of the surface. However, in large areas on the Si surface, the blisters appear self-ordered. In *Figure 2* a grid was drawn on the picture to highlight the 2D lattice formed by the blisters on Si(100) substrate. It can be observed that they are positioned on top of a diamond of approximately  $55 \mu\text{m}$  as unit cell. On glass the blisters are not ordered and do not present the characteristic circular aspect (*Figure 3 b*), emphasizing the substrate influence. As a hypothesis, this pattern indicates a possible influence of the crystal structure of the Si(100), and hence of the surface energy of the substrate, even if the native oxide was not etched in the cleaning procedure. Indeed, the  $60^\circ$  parallelograms observed could be due to the substrate structure. As a result of the processing required to prepare the Si(100) wafers, the surface of the substrate exhibits typical imperfections such as steps and ledges that separate the terraces of the atomic Si planes (Butt et al., 2006; Franssila, 2010). This is particularly true when using Si(100) substrate misoriented of  $3^\circ$  as in the present work, *i.e.* the growth occurs on a (100) vicinal surface.

On these Si substrates, the emergence of perfect  $60^\circ$  dislocations was reported (Godet et al., 2002). This orientation is also commonly encountered in epitaxial growth (Liu and Santos, 1999). Furthermore, steps and grooves are also observed by AFM for the native oxide layers present on semiconducting films deposited by MOCVD (Bluhm et al., 1994). The steps and grooves on the native oxide are associated to a relaxation of the strained layers that occurs during the film growth (Bluhm et al., 1994), and probably in this case during the Si(100) cutting process. The  $60^\circ$  angle observed in *Figure 2* for the blisters orientation could be thus indicative of a preferential heterogeneous nucleation of the blisters at the sites of Si(100) wafer. Such steps were previously observed by AFM for bare Si(100) substrates and Si(100) substrates coated with PMMA (Manole et al., 2013).

For our experiments achieved with 2% HCHPK by Photo-DLICVD it seems that the UV activation of the gas phase is not sufficiently efficient for a high activation of monomer molecules. As a result both non-activated and photo-activated monomers condense on the surface of the substrate and lead subsequently to blisters and PPy thin film, respectively. Notably, the pulsed flow of the monomer/carrier gas can be an important factor in the kinetics of these two parallel mechanisms. In a previous work we provided physical means to release the liquid monomer encapsulated into PMMA polymer coatings by a Thermally Induced-

Release of the Internal Phase (TI-RIP) process (Manole et al., 2012). In the present paper to prevent the presence of liquid microdroplets of monomer, the photo-activation of the gas phase will be chemically enhanced to increase the polymerization kinetics in order to obtain only a solid polymeric film of PPy on the substrate. To achieve this, a pyrrole solution with  $\text{AgNO}_3$  was made, while the HCHPK content was increased to 3%.

### 3.2. Extrinsicly doped PPy films

According to the literature, the conductivity of undoped PPy films is around  $10^{-12}$  S/cm making it a good electrical insulator (Allcock, 2011). By chemical doping of the PPy films the conductivity can reach the order of magnitude of silver (Allcock, 2011). The PPy doped with a wide range of anions belongs to a class of Intrinsic Conductive Polymers (ICPs) (Joo and Epstein, 1994; Otero and Sansiñena, 1995; Wang and Jing, 2005). The main characteristic of the ICPs is that the excitation generates directly the production of free carriers (Aldissi, 1993). In these experimental runs, the anion  $\text{NO}_3^-$  dissolved in the monomer (Murphy et al., 2001) from the  $\text{AgNO}_3$  salt and acts as anion dopant of PPy. A study on the intrinsic doping of PPy films was treated in other work (Pirvu et al., 2011). The PPy requires conformational changes to accommodate the extra charges of the anions. These changes can be investigated by Raman mainly by following the C=C stretching bonds that are mainly related to the redox state of PPy (Nguyen Thi Le et al., 2004). In Figure 4, the C=C stretching frequency shifts over  $1600\text{ cm}^{-1}$  (noted cation species) are associated to conductive species of PPy doped with  $\text{NO}_3^-$  (Santos et al., 2007). Also the reduced states of the PPy associated to the presence of undoped PPy are observed around  $1570\text{ cm}^{-1}$  (noted reduced species in the figure 3) (Santos et al., 2007). Clearly, the most predominant character is the one of the conductive species ( $\sim 1600\text{ cm}^{-1}$ ), also confirmed at  $930\text{ cm}^{-1}$  in the Raman spectra (Santos et al., 2007).

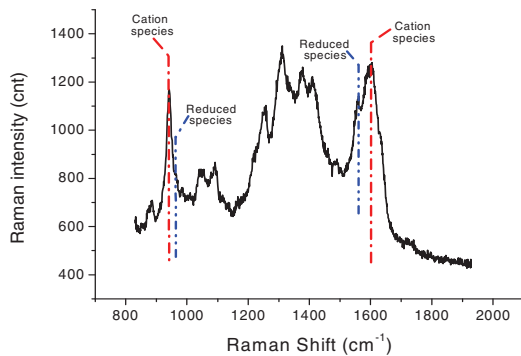


Figure 4: Surface Enhanced Raman spectra of the PPy/Ag thin film grown by Photo-DLICVD. The cation species represent the doped PPy while the reduced species represent the undoped state.

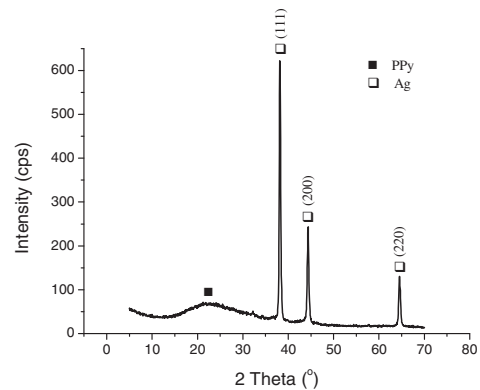


Figure 5: X-ray diffraction of a PPy/Ag film deposited on glass. The amorphous PPy gives a broad peak centered at 22 deg and the Ag NPs orientations are indicated.

An important feature of the Raman spectra is that it presents an enhancement of the band intensity that allows a clear separation of the bands. This effect, called Surface Enhanced Raman Spectroscopy (SERS), can be achieved by the presence of Ag nanoparticles that generate a plasmonic field at the metal/polymer interface (Hossain et al., 2009). The Ag NPs must exhibit a diameter between 20 and 200 nm to generate the SERS effect (Bell and McCourt, 2009).

The growth of Ag nanoparticles in our PPy films results from the  $\text{AgNO}_3$  salt dissolved into the liquid monomer injected into the CVD reactor. The nitrate anions act as intrinsic doping for PPy and the cations  $\text{Ag}^+$

serves as sources for Ag NPs. The presence of Ag is known to increase the PPy film conductivity considerably (Alqudami et al., 2007; Nghia and Tung, 2009; Wei et al., 2009). Due to the direct role that Ag plays in the PPy carrier yield, the PPy/Ag NPs films obtained by Photo-DLICVD belong to the Extrinsic Conductive Polymers (ECPs) class (Aldissi, 1993).

The Ag NPs exhibit the crystalline structure of metal silver as shown by the XRD pattern of PPy/Ag thin film in Figure 5. In the analyzed angular range, three narrow diffraction peaks were found at 2.359, 2.040 and 1.444 Å, which correspond to the (111), (200) and (220) orientations of the fcc cubic structure of Ag NPs. These values are similar to the Ag NPs grown under photo-polymerization in wet conditions (Hodko, Gamboa-Aldeco, and O. Murphy, 2009).

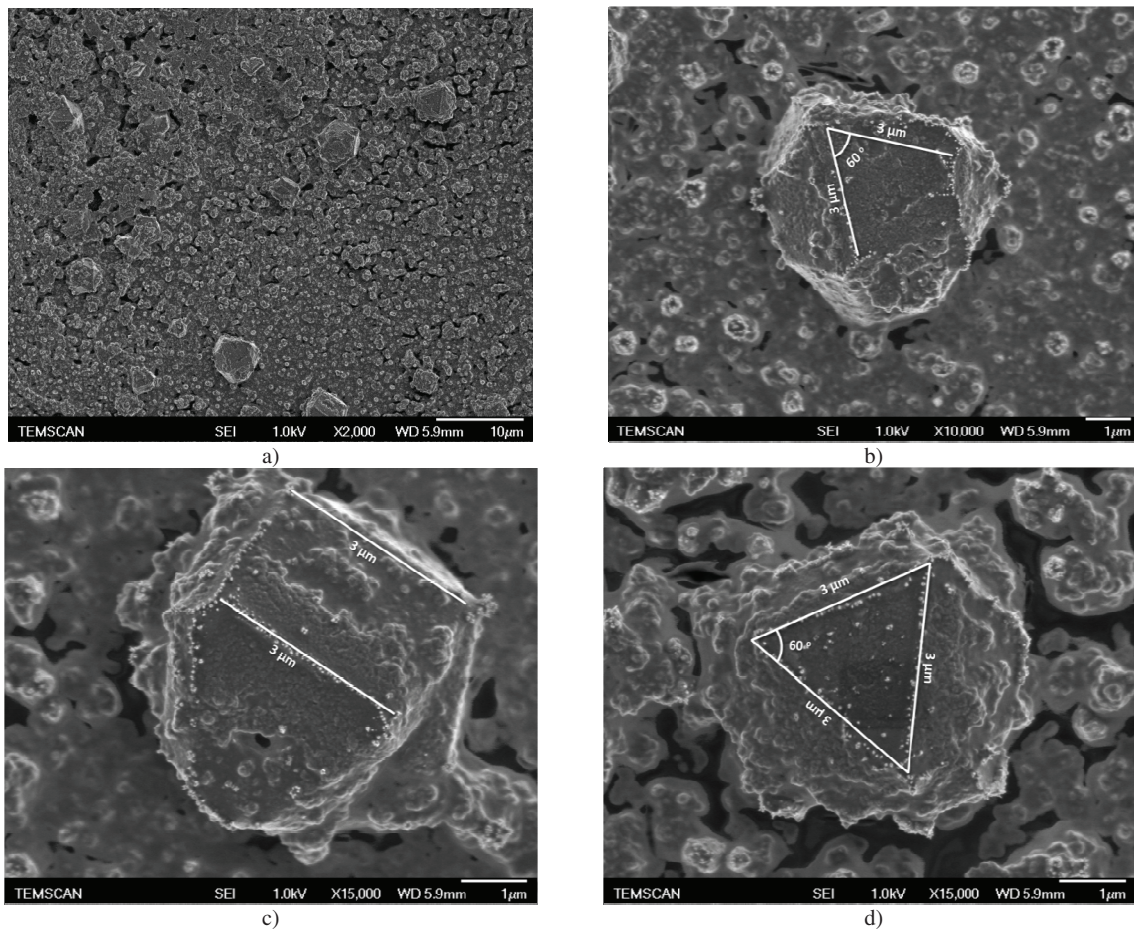


Figure 6: FESEM micrographs of a wide surface area (a) and of facet-like arrangements of the Ag NPs at higher magnification (b, c, d). The geometrical parameters of some particle-like PPy/Ag composite (average size 3 – 5 μm) are highlighted; Ag NPs (40 nm) are linearly self-ordered on the ledges of the facets of these composite particles.

A broad hump centered at approximately 4.0 Å (2 theta = 22 deg) could be assigned to the amorphous PPy film because it was not observed on the bare glass substrate. Comparatively the d-spacing for electrochemically polymerized PPy was reported at around 3.5 Å (Buckley et al., 2003) for a similar sized ClO<sub>4</sub><sup>-</sup> anion (Kielland, 1937). This weak XRD peak is characteristic of the π-stacking of amorphous PPy leading to a short range order even if the material is globally amorphous (Xing and Zhao, 2007). For the wet

photo-polymerization achieved at atmospheric pressure, similar d-spacing was reported (Hodko, Gamboa-Aldeco, and O. Murphy, 2009; Hodko, Gamboa-Aldeco, and O.J. Murphy, 2009), indicating that the low pressure conditions of Photo-DLICVD does not have a significant influence on the PPy d-spacing. Therefore the presence of the silver grains could explain the increased packing distance of PPy and confirms the nature of the deposited films as ECP (Hodko, Gamboa-Aldeco, and O. Murphy, 2009).

By contrast with undoped PPy layers, FESEM analysis of Ag-doped PPy thin films did not show afterimage at moderate acceleration voltages of the primary electron beam, indicating the material exhibits a sufficient conductivity to be readily observed without metallization.

It is remarkable that no blister is observed in PPy/Ag thin films. This reveals a higher efficiency in the polymerization reaction. Silver is intimately mixed with PPy but it form grains whose the biggest size reaches of 3-5  $\mu\text{m}$ . At higher magnification, Ag nanoparticles of diameters around 40 nm can be observed on facets of the biggest grains (Figure 6 *b, c, d*). This nanometric size of Ag particles is consistent with the SERS effect observed in Raman analysis. Curiously, the grains present facet-like morphologies characteristic of a crystal (Figure 6 and magnified in Figure 6 *b, c, d*). The presence of the  $\text{Ag}^+$  could not only influence the d-spacing, but it could also lead to an ordered growth of PPy/Ag NPs hybrid films. In previously reported conditions of Ag deposition by evaporation on a PPy film, a strong hybridization was found for the Ag d-electrons and the orbitals of PPy by the formation of a PPy/Ag alloy (Mikalo et al., 2001). Such an alloying effect is probably occurring during the CVD growth of the PPy/Ag films under low pressure conditions. In CVD the intermolecular forces are likely to play an important role in the surface diffusion of the molecules before the heterogeneous reaction. A series of molecular-mediated assemblies of Ag NPs were already reported in the literature (Mallick et al., 2005; Filippo et al., 2009; Maayan and Liu, 2011; Park et al., 2013). However this hybrid growth of the PPy/Ag NPs by Photo-DLICVD leads to reproducible 3  $\mu\text{m}$  length of NPs arrangement along the ledges of the facets of the biggest grains. This linear arrangement leads to 2D ordering on the facets (such as the equilateral triangle in Figure 6 *d*) and to a more complex 3D arrangement by considering several facets of a grain (observed in Figure 6 *b, c*). To our knowledge such effect of the hybridization in PPy/Ag films had not been previously observed in a CVD process.

#### 4. Conclusions

Undoped PPy and extrinsic doped PPy/Ag thin films were deposited by an original Photo-DLICVD process. The undoped PPy films exhibit an insulator behavior when they are observed by SEM. The AFM showed a conformal deposition over blisters and Si(100) surface. The blister formation occurs during the CVD growth and originates from an insufficient photo-activation of the monomers molecules in the gas phase that condense on the surface of the substrate. Interestingly a self-ordering of the blisters was observed on some parts of the Si(100) substrate. On the glass substrate the blisters were irregular and not ordered. As first hypothesis, this was associated to the heterogeneous nucleation at defects possibly induced by the structure of vicinal surface of Si(100) substrate.

Hybrid PPy/Ag thin films were grown in one step by dissolving  $\text{AgNO}_3$  in the liquid solution injected in the CVD reactor. No blister was found in these nanocomposite polymeric coatings. Evidence for the formation of metallic Ag NPs was given by XRD patterns. The efficiency of the anion doping was deduced from Raman analysis and in particular by the SERS effect induced by the Ag NPs. Silver is intimately mixed with the polymer film. The PPy/Ag NPs hybrid material forms faceted grains with a micrometric size. Unlike for the undoped PPy films, SEM analysis gave evidence for a conducting behavior of these Ag-doped PPy coatings. Conductivity measurements should confirm this shortly. A linear arrangement of Ag NPs was observed on the ledges of these faceted grains forming a 2D ordering on each facet. However a more complex 3D arrangement of Ag NPs was found by considering several facets with different orientations.

## References

- Ahn, S. D., S. Y. Kang, Y. E. Lee, M. J. Joung, C. A. Kim, and K. S. Suh, 2003, Thin Film Morphology and Growth Mechanism of Pentacene Thin Film Using Low-Pressure Organic Vapor Deposition: MRS Online Proceedings Library, 769, p. H6.19.
- Ahn, S., S. Y. Kang, J. Y. Oh, K. S. Suh, K. I. Cho, and J. B. K. F., 2012, Pressure Control Organic Vapor Deposition Methods for Fabricating Organic Thin-Film Transistors: ETRI Journal, 34, p. 970.
- Aldissi, M., 1993, Intrinsicly Conducting Polymers: An Emerging Technology: Springer, p. 246.
- Allcock, H. R., 2011, Introduction to Materials Chemistry: John Wiley & Sons, p. 388.
- Alqudami, A., S. Annapoorni, P. Sen, and R. S. Rawat, 2007, The incorporation of silver nanoparticles into polypyrrole: Conductivity changes: Synthetic Metals, 157, p. 53.
- Angeli, A., and L. Alessandri, 1916, The electrochemistry of conducting polymers: Gazz. Chim. Ital, 46, p. 279.
- Bakar, S. A., S. T. Hussain, and M. Mazhar, 2012, CdTiO<sub>3</sub> thin films from an octa-nuclear bimetallic single source precursor by aerosol assisted chemical vapor deposition (AACVD): New Journal of Chemistry, 36, p. 1844.
- Bell, S. E. J., and M. R. McCourt, 2009, SERS enhancement by aggregated Au colloids: effect of particle size: Physical Chemistry Chemical Physics, 11, p. 7455.
- Bluhm, H., U. D. Schwarz, F. Herrmann, and P. Paufler, 1994, Study of the influence of native oxide layers on atomic force microscopy imaging of semiconductor surfaces: Applied Physics A, 59, p. 23.
- Boisselier, G., F. Maury, and F. Schuster, 2013, SiC coatings grown by liquid injection chemical vapor deposition using single source metal-organic precursors: Surface and Coatings Technology, 215, p. 152.
- Buckley, L. J., D. K. Roylance, and G. E. Wnek, 2003, Influence of dopant ion and synthesis variables on mechanical properties of polypyrrole films: Journal of Polymer Science Part B: Polymer Physics, 25, p. 2179.
- Butt, H.-J., K. Graf, and M. Kappl, 2006, Physics and Chemistry of Interfaces: John Wiley & Sons, p. 375.
- Cao, G., 2004, Nanostructures & Nanomaterials: Synthesis, Properties & Applications: Imperial College Press, p. 452.
- Chan, K., L. E. Kostun, W. E. Tenhaeff, and K. K. Gleason, 2006, Initiated chemical vapor deposition of polyvinylpyrrolidone-based thin films: Polymer, 47, p. 6941.
- Crick, C. R., J. C. Bear, A. Kafizas, and I. P. Parkin, 2012, Superhydrophobic Photocatalytic Surfaces through Direct Incorporation of Titania Nanoparticles into a Polymer Matrix by Aerosol Assisted Chemical Vapor Deposition: Advanced Materials, 24, p. 3505.
- Dall'Olio, A., G. Dascola, V. Varacco, and V. Bocchi, 1968, Electron paramagnetic resonance and conductivity of an electrolytic oxypyrrole [(pyrrole polymer)] black: CR Acad Sci Ser C, 267, p. 433.
- Das, A., M. Frenkel, N. A. M. Gadalla, S. Kudchadker, K. N. Marsh, A. S. Rodgers, and R. C. Wilhoit, 1993, Thermodynamic and Thermophysical Properties of Organic Nitrogen Compounds. Part II. 1□ and 2□Butanamine, 2□Methyl□1□Propanamine, 2□Methyl□2□Propanamine, Pyrrole, 1□,2□, and 3□Methylpyrrole, Pyridine, 2□,3□, and 4□Methylpyridine, Pyrrolidine, Piperidine, Indole, Quinoline, Isoquinoline, Acridine, Carbazole, Phenanthridine, 1□ and 2□Naphthalenamine, and 9□Methylcarbazole: Journal of Physical and Chemical Reference Data, 22, p. 659.
- Diaz, A. F., K. K. Kanazawa, and G. P. Gardini, 1979, Electrochemical polymerization of pyrrole: Journal of the Chemical Society, Chemical Communications, p. 635.
- Douard, A., C. Bernard, and F. Maury, 2008, Thermodynamic simulation of atmospheric DLI-CVD processes for the growth of chromium-based hard coatings using bis(benzene)chromium as molecular source: Surface and Coatings Technology, 203, p. 516.
- Douard, A., and F. Maury, 2006, Nanocrystalline chromium-based coatings deposited by DLI-MOCVD under atmospheric pressure from Cr(CO)<sub>6</sub>: Surface and Coatings Technology, 200, p. 6267.
- Edusi, C., G. Sankar, and I. P. Parkin, 2012, The Effect of Solvent on the Phase of Titanium Dioxide Deposited by Aerosol-assisted CVD: Chemical Vapor Deposition, 18, p. 126.
- Filippo, E., A. Serra, and D. Manno, 2009, Self-assembly and branching of sucrose stabilized silver nanoparticles by microwave assisted synthesis: From nanoparticles to branched nanowires structures: Colloids and Surfaces A: Physicochemical and Engineering Aspects, 348, p. 205.
- Franssila, S., 2010, Introduction to Microfabrication: John Wiley & Sons, p. 535.
- Godet, J., L. Pizzagalli, S. Brochard, and P. Beauchamp, 2002, Surface step effects on Si (100) under uniaxial tensile stress, by atomistic calculations: Scripta Materialia, 47, p. 481.
- Hodko, D., M. Gamboa-Aldeco, and O. J. Murphy, 2009, Photopolymerized silver-containing conducting polymer films. Part I. An electronic conductivity and cyclic voltammetric investigation: Journal of Solid State Electrochemistry, 13, p. 1063.
- Hodko, D., M. Gamboa-Aldeco, and O. J. Murphy, 2009, Photopolymerized silver-containing conducting polymer films. Part II. Physico-chemical characterization and mechanism of photopolymerization process: Journal of Solid State Electrochemistry, 13, p. 1077.
- Hossain, M. K., Y. Kitahama, G. G. Huang, X. Han, and Y. Ozaki, 2009, Surface-enhanced Raman scattering: realization of localized surface plasmon resonance using unique substrates and methods: Analytical and Bioanalytical Chemistry, 394, p. 1747.
- Jones, A. C., and M. L. Hitchman, 2009, Chemical Vapor Deposition: Precursors, Processes and Applications: Royal Society of Chemistry, p. 600.
- Joo, J., and A. J. Epstein, 1994, Electromagnetic radiation shielding by intrinsically conducting polymers: Applied Physics Letters, 65, p. 2278.
- Kielland, J., 1937, Individual activity coefficients of ions in aqueous solutions: Journal of American Chemical Society, 4, p. 4.
- Liu, W. K., and M. B. Santos, 1999, Thin Films: Heteroepitaxial Systems: World Scientific, p. 708.

- Maayan, G., and L.-K. Liu, 2011, Silver nanoparticles assemblies mediated by functionalized biomimetic oligomers: *Peptide Science*, 96, p. 679.
- Malinauskas, A., 2001, Chemical deposition of conducting polymers: *Polymer*, 42, p. 3957.
- Mallick, K., M. J. Witcomb, and M. S. Scurrill, 2005, Self-assembly of silver nanoparticles in a polymer solvent: formation of a nanochain through nanoscale soldering: *Materials Chemistry and Physics*, 90, p. 221.
- Manole, C. C., O. Marsan, C. Charvillat, I. Demetrescu, and F. Maury, 2013, Evidences for liquid encapsulation in PMMA ultra-thin film grown by liquid injection Photo-CVD: *Progress in Organic Coatings*, DOI: <http://dx.doi.org/10.1016/j.porgcoat.2013.05.027>
- Manole, C. C., F. Maury, and I. Demetrescu, 2012, Thermally Induced Release of Internal Liquid Phase Encapsulated in a Polymer Membrane Grown by Photoactivated DLICVD: *Chemical Vapor Deposition*, 18, p. 274.
- Maury, F., A. Douard, S. Delclos, D. Samelor, and C. Tendero, 2009, Multilayer chromium based coatings grown by atmospheric pressure direct liquid injection CVD: *Surface and Coatings Technology*, 204, p. 983.
- Mikalo, R. P., G. Appel, P. Hoffmann, and D. Schmeißer, 2001, Band bending in doped conducting polypyrrole: interaction with silver: *Synthetic Metals*, 122, p. 249.
- Mohammadi, A., M.-A. Hasan, B. Liedberg, I. Lundström, and W. R. Salaneck, 1986, Chemical vapour deposition (CVD) of conducting polymers: Polypyrrole: *Synthetic Metals*, 14, p. 189.
- Mungkalasiri, J., L. Bedel, F. Emieux, J. Doré, F. N. R. Renaud, and F. Maury, 2009, DLI-CVD of TiO<sub>2</sub>-Cu antibacterial thin films: Growth and characterization: *Surface and Coatings Technology*, 204, p. 887.
- Murphy, O. J., G. D. Hitchens, D. Hodko, E. T. Clarke, D. L. Miller, and D. L. Parker, 2001, Method of forming electronically conducting polymers on conducting and ..., 6210537.
- Nghia, N. D., and N. T. Tung, 2009, Preparation and characterization of hybrid materials based on polypyrrole and silver nanoparticles: *Journal of Physics: Conference Series*, 187, p. 012050.
- Nguyen Thi Le, H., M. . Bernard, B. Garcia-Renaud, and C. Deslouis, 2004, Raman spectroscopy analysis of polypyrrole films as protective coatings on iron: *Synthetic Metals*, 140, p. 287.
- Otero, T. F., and J. M. Sansiñena, 1995, Artificial muscles based on conducting polymers: *Bioelectrochemistry and Bioenergetics*, 38, p. 411.
- Ozaydin-Ince, G., A. M. Coclite, and K. K. Gleason, 2012, CVD of polymeric thin films: applications in sensors, biotechnology, microelectronics/organic electronics, microfluidics, MEMS, composites and membranes: *Reports on Progress in Physics*, 75, p. 016501.
- Ozaydin-Ince, G., and K. K. Gleason, 2010, Tunable Conformality of Polymer Coatings on High Aspect Ratio Features: *Chemical Vapor Deposition*, 16, p. 100.
- Park, J.-H., 2001, *Chemical Vapor Deposition*: ASM International, p. 477.
- Park, W., K. Emoto, Y. Jin, A. Shimizu, V. A. Tamma, and W. Zhang, 2013, Controlled self-assembly of gold nanoparticles mediated by novel organic molecularcages: *Optical Materials Express*, 3, p. 205.
- Pirvu, C., C. C. Manole, A. B. Stoian, and I. Demetrescu, 2011, Understanding of electrochemical and structural changes of polypyrrole/polyethylene glycol composite films in aqueous solution: *Electrochimica Acta*, 56, p. 9893.
- Santos, M. J. L., A. G. Brolo, and E. M. Girotto, 2007, Study of polaron and bipolaron states in polypyrrole by in situ Raman spectroelectrochemistry: *Electrochimica Acta*, 52, p. 6141.
- Santucci, V., F. Maury, and F. Senocq, 2010, Vapor phase surface functionalization under ultra violet activation of parylene thin films grown by chemical vapor deposition: *Thin Solid Films*, 518, p. 1675.
- Shah, A. Y., A. Wadawale, V. S. Sagoria, V. K. Jain, C. A. Betty, and S. Bhattacharya, 2012, Aerosol assisted chemical vapour deposition of germanium thin films using organogermanium carboxylates as precursors and formation of germania films: *Bulletin of Materials Science*, 35, p. 365.
- Wang, Y., and X. Jing, 2005, Intrinsically conducting polymers for electromagnetic interference shielding: *Polymers for Advanced Technologies*, 16, p. 344.
- Wei, Y., L. Li, X. Yang, G. Pan, G. Yan, and X. Yu, 2009, One-Step UV-Induced Synthesis of Polypyrrole/Ag Nanocomposites at the Water/Ionic Liquid Interface: *Nanoscale Research Letters*, 5, p. 433.
- Weiss, F. et al., 2000, Injection MOCVD: ferroelectric thin films and functional oxide superlattices: *Surface and Coatings Technology*, 133-134, p. 191.
- Xing, S., and G. Zhao, 2007, One-step synthesis of polypyrrole-Ag nanofiber composites in dilute mixed CTAB/SDS aqueous solution: *Materials Letters*, 61, p. 2040.
- Xu, J., A. Asatekin, and K. K. Gleason, 2012, The Design and Synthesis of Hard and Impermeable, Yet Flexible, Conformal Organic Coatings: *Advanced Materials*, 24, p. 3692.